Journal of Casting & Materials Engineering Vol. 9 No. 3 (2025) 39–44
https://doi.org/10.7494/jcme.2025.9.3.39

Design of a Solidification Rate Measurement Experiment for Cast Steel in Molds Made of Different Sands Using Computer Simulation

Natalia Mordyl [a*], Jarosław Jakubski [a], Paweł Leszek Żak [a]

[a]AGH University of Krakow, Faculty of Foundry Engineering, 23 Reymonta St., 30-059 Krakow, Poland
e-mail: mordyl@agh.edu.pl

Received: 9 July 2025/Accepted: 8 August 2025/Published online: 18 September 2025.
This article is published with open access at AGH University of Science and Technology Journals.

Abstract

This article presents the design process of the casting technology for a step-shaped casting made of steel using simulation tools. A series of proposals for gating and feeding systems were simulated in the MAGMASoft® software. Results of numerical simulations allowed the Authors to select the casting technology which allows defect-free casting to be obtained. A numerical analysis of the cooling rate of a step-shaped casting made of GX70CrMnSiNiMo2 tool steel with a 5% Ti addition was carried out for the selected manufacturing technology. Due to the nature of the material used and the extended presence of martensite during cooling, in-mold hardening of the casting may occur. The simulations showed that the type of molding material affects the cooling rate, which is confirmed by the analysis of cooling curves and the morphology of shrinkage porosity. The analysis of solidification rates provides a valuable starting point and basis for subsequent research stages, taking into account the actual properties of the molding sands and the phase transformations occurring in the selected steel type. The casting technology design, which ensures the production of sound casting, was developed as part of this study. A series of simulations using different molding materials confirms the significant impact that the choice of mold material has on the casting solidification and cooling process.

Keywords:

cooling rate, molding materials, GX70CrMnSiNiMo2 tool steel, numerical simulation

1. INTRODUCTION

Technological advancements and increasing market demands require machines and equipment which operating under conditions of intense abrasive wear, enhanced durability and reliability. In order to extend the service life of tools technological solutions that provide increased resistance to abrasive wear are being sought. However, for many structural materials, improvements achieved through changes in chemical composition, phase composition, or conventional heat treatment are insufficient [1].

Recent literature has reported growing interest in technological approaches aimed at strengthening the matrix by secondary carbide precipitation. The appropriate type, shape, and distribution of carbides significantly improve the wear resistance of alloys containing carbide-forming elements such as titanium, vanadium, niobium, or chromium, as highlighted in various studies [2–10].

Despite the understanding of wear mechanisms, universal material selection criteria based on operating conditions have yet to be developed, mainly due to the still-unexplained correlation between microstructure and resistance to abrasive wear – even though it is well known that microstructure plays a crucial role in shaping tribological properties [11].

The microstructure of alloys is influenced by technological factors related to mold preparation, liquid metal treatment, the rate of solidification, as well as the type and parameters of the applied heat treatment [12]. In newly developed alloys, the relationships between chemical composition, microstructure, and the heat flow through the mold have not been fully studied – particularly in the context of high-alloyed tool steels with increased abrasive wear resistance and higher contents of carbide-forming elements such as chromium, molybdenum, and titanium. Since these correlations have been thoroughly examined for gray cast iron, analyzing the influence of molding materials on the microstructure and properties of tool steels is of particular importance [13–16]. The aim of this study is to design an experiment that will contribute to expanding knowledge in this area.

The use of numerical methods based on the discrete approximation of Fourier–Kirchhoff partial differential equations for heat transfer allows the analysis of how molding materials affect the run of the cooling and solidification process of metal within the mold cavity [17, 18]. Although the models used in simulations may be subject to certain inaccuracies and do not always take into account all real processes, the simulation results allow for the prediction

of technological process behavior. This makes it possible to develop optimal production solutions without the need for costly experimental trials. For this reason, modern engineers and researchers are increasingly turning to simulation tools as support in developing manufacturing processes. Such an approach has been adopted by the Authors of this study.

2. MATERIALS AND METHODS

The model of the step-shaped casting was created using the "Geometry" module of the MAGMASoft® software. This module allows its user to make 3D geometries as in a CAD system, which are subjected to operations necessary to create a numerical model. Several variants of the casting technology were proposed and the quality of the resulting casting was analyzed for each variant. Computer simulations were conducted in MAGMASoft® (educational-research version, License ID: 433400). The calculations in the MAGMASoft® program are performed using the Finite Difference Method (FDM).

For the numerical analysis, a virtual step-shaped casting was used, featuring four wall thicknesses: 5 mm, 15 mm, 25 mm, and 50 mm, consisting of the main part and a technological allowance (overpour). The length of each step was 50 mm, and the width was 48 mm. The dimensions of the casting mold were 260 × 450 × 270 mm^3. Based on a literature review, the cooling analysis was carried out for a precipitation-hardened tool steel characterized by the highest resistance to abrasive wear in the Miller test, namely GX70CrMnSiNiMo2 steel with an addition of 5% titanium (Table 1) [10]. Solidification simulations were performed for both first- and second-generation molding sands. In first-generation sands with bentonite, the base material consisted of quartz and olivine sand. In second-generation sands – prepared using the self-hardening molding sands with the furfuryl binder – quartz, chromite, and Cerabeads 650 sands (sintered mullite with a low linear expansion coefficient) were used as the base material. The data for determining the thermophysical coefficients of the molding materials were obtained from the MAGMASoft® database. In this database, the values of parameters are tabularly defined for various temperature values. The program, using appropriate approximations, calculates the temperature-dependent thermophysical parameters in each cell of the computational domain base on its local temperature.

The heat accumulation coefficient of molding sand is the material parameter that indicates how much heat the molding sand can draw from an alloy poured into the mold cavity, it is given by Equation (1):

$$b_2 = \sqrt{\lambda \cdot \rho \cdot c_p} \tag{1}$$

where:

b_2 – heat accumulation coefficient of molding sand [(W s^{½})/(m^2 K)],
λ – heat transfer coefficient [W/(m K)],
ρ – density [kg/m^3],
c_p – specific heat [J/(kg K)].

Having access to the values of the thermophysical parameters for molding materials stored in the MAGMASoft® database, it is possible to determine the heat accumulation coefficient values for the specified temperature values. Such calculations, aimed at showing the extent to which the selected molding materials differ in this value and how they change with increasing temperature, were carried out by the authors and the results are presented in Table 2.

Identical process parameters were assumed for each design variant, namely an initial mold temperature of 20°C and a pouring temperature of 1550°C, thereby minimizing the number of variables affecting the cooling rate. Other simulation settings are collected in Table 3.

Table 1
Chemical composition of standard and titanium-modified GX70CrMnSiNiMo2 alloy [10]

Alloy designation	Chemical composition [wt. %]										
	C	Mn	Si	P	S	Cr	Ni	Mo	V	Al	Ti
Standard GX70CrMnSiNiMo2	0.60–0.75	0.90–1.05	<0.55	<0.04	<0.04	1.80–1.95	0.60–0.80	0.40–0.50	–	–	–
Ti-modified alloy	1.78	0.96	1.75	0.02	0.04	1.10	0.90	0.30	0.20	0.02	0.50

Table 2
Values of heat accumulation coefficients calculated on the base of MAGMASoft® database temperature-dependent thermophysical coefficients

Mold material	Temperature [°C]		
	100	400	700
	Heat accumulation coefficient [(W s^{½})/(m^2 K)]		
Quartz-furan	1021	1080	1101
Quartz-bentonite	1100	1049	1062
Chromite-furan	1522	1482	1508
Olivin-bentonite	1035	1161	1243
Cerabeads-furan	489	588	692

Table 3
Casting process parameters used for to set casting simulation project in MAGMASoft®

Process parameter	Value
Theoretical pouring time [s]	8.5
Simulation pouring time [s]	5
Pouring rate [cm^3/s]	120
Mold initial temperature [°C]	20
Cast alloy initial temperature [°C]	1550

According to the project assumptions, the casting was divided into two parts (main casting and casting allowance) in such a way that, in the case of vertical pouring, all shrinkage defects would concentrate in the technological allowance. The technological allowance had the shape of a cube with dimensions of 48 × 70 × 50 mm^3. However, the proposed solution did not meet the expected results (Fig. 1). Due to ergonomic considerations related to mold preparation, it was decided to simulate a horizontal pouring variant (Fig. 2).

Because of the morphology of the shrinkage porosity, it was necessary to use feeders to obtain a defect-free final casting while minimizing the amount of casting alloy used. For this purpose, both commercial feeders from FOSECO and custom-designed solutions were employed (Fig. 3).

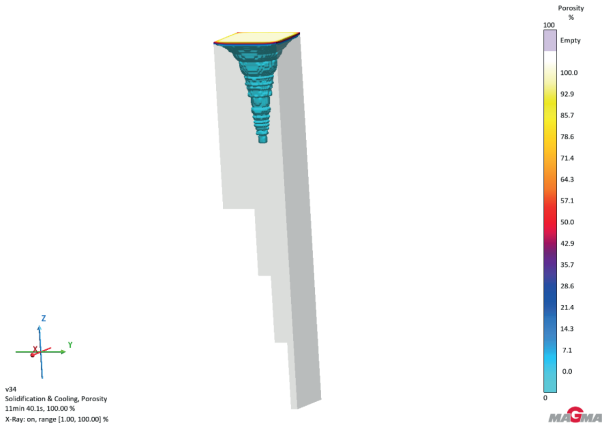

Fig. 1. Distribution of the porosity in the casting while pouring verticaly

Fig. 2. Distribution of the porosity in the casting while pouring horizontaly

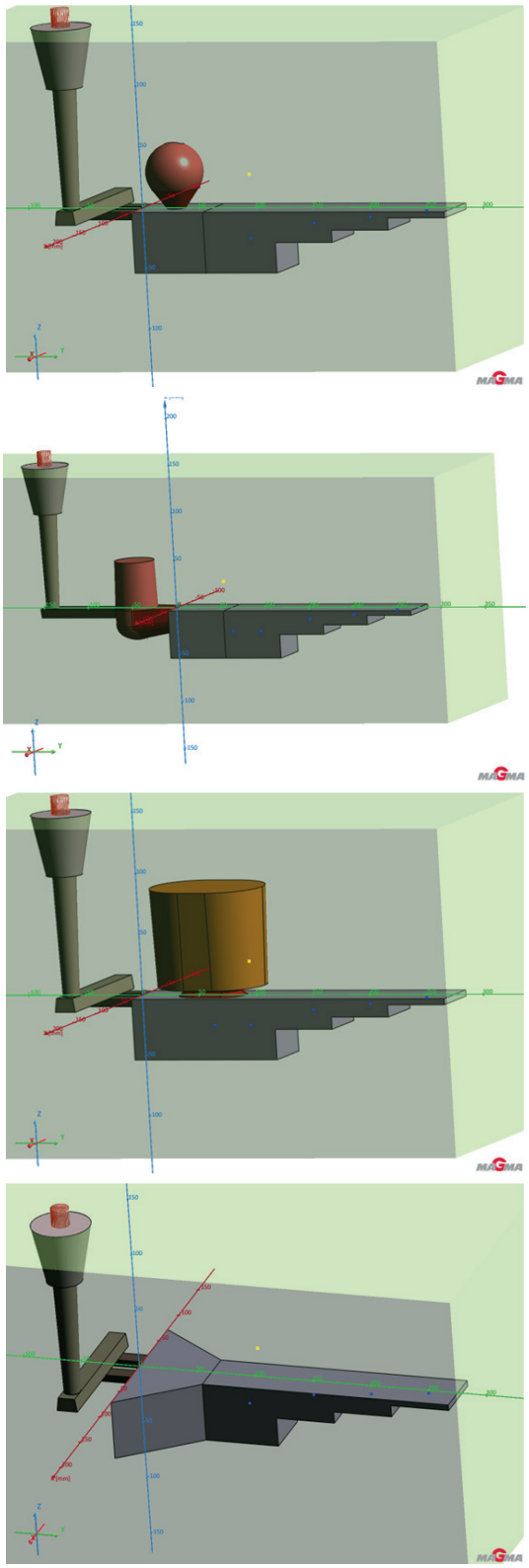

Fig. 3. Examples of tested casting filling and feeding systems

The analyzed technological variants – 31 configurations differing in the method of filling mold cavity and the type of feeders used – allowed for the selection of a solution that ensured the highest yield and the absence of porosity in the functional part of the casting (Fig. 4). The volume of the feeder along with the feederneck that was finally chosen was 66.130 mm^3.

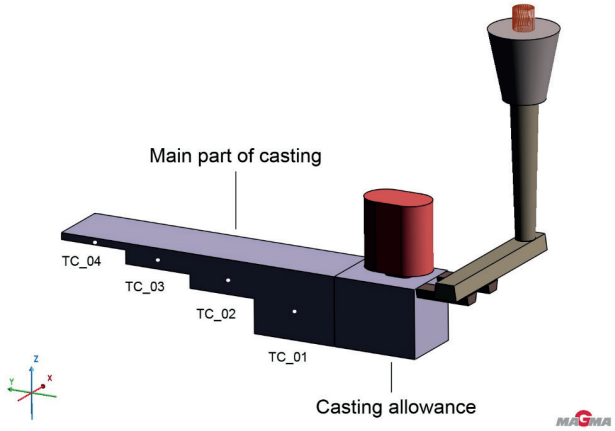

Fig. 4. Chosen technological variant, that ensure high yield and defect-free casting

In the central part of each segment of the casting (different wall thickness), one thermocouple (TC_01-TC_04) was placed (Fig. 4), which enabled the recording of the cooling curves. On this basis, correlations between the cooling rate, wall thickness, and the used molding material were determined.

3. RESULTS

The simulations conducted within this work made it possible to evaluate the casting technology variants in terms of the size and location of shrinkage porosity. Based on this analysis, a filling and feeding system design was selected that enables the production of a defect-free casting with a yield of 69.1%.

The selected casting design was subjected to further studies involving simulations performed using different molding materials. The thermophysical parameters of the molding materials used in the analysis were taken from the built-in database of the simulation software. The authors are aware that these parameters refer to reference molding materials; therefore, to improve the accuracy of the modelling results, future research will include testing of molding sands based on the actual base materials selected for the simulations and used by the Authors in their work.

Virtual thermocouples were placed in the mold cavity to record temperature changes at the centers of regions with defined wall thicknesses. The cooling rate analysis revealed significant differences depending on both the wall thickness of the casting and the type of molding material used (Fig. 5). Calculated cooling rates as well as crystallization times in centers the thinnest and the thickest step segment of the casting are presented in the Table 4. It is well known that the greater the mold's ability to accumulate heat, the coarser the grain size of the casting, which negatively affects its performance properties [12, 19, 20]. Digitizing the cooling curves, combined with economic considerations, allows for the selection of the most optimal variant in terms of grain refinement and manufacturing technology.

The obtained results indicate that the molding materials have an impact on the solidification rate. The planned further examination, that among others will include extending the scope of temperature measurements to include the final phase transformations, could allow for the prediction of the final microstructure of the cast steel component. The studied alloy is characterized by a wide range of martensitic transformation. However, the diffusionless transformation of austenite in the mold – due to rapid cooling – can lead to significant internal stresses and cracking. Additionally, the casting geometry, which causes variations in the cooling rate in different parts (between following steps), may lead to the inhibition of casting shrinkage and generate stresses in the castings, that may lead to hot cracks, the appearance of which further increases the number of cracks and casting production costs.

The type of molding material also influenced the shape and size of shrinkage porosity in the allowance (Fig. 6). A correlation was observed between the cooling rate and the shape of porous regions – the slower the cooling, the more elongated the porous volume. Due to the generalized properties of the first- and second-generation sands in the MAGMASoft® program, it is necessary to determine the actual parameters of the molding materials so that the virtual data can be as close as possible to the real conditions.

Table 4
Numerically simulated cooling rates and crystallization rates in centers of the thinnest and thickest casting step segment

Mold material	Cooling rate [K/s]		Crystallization time [s]	
	Min	max	min	max
Quartz-furan	0.236	11.530	31.61	290.50
Quartz-bentonite	0.214	11.213	28.85	240.40
Chromite-furan	0.270	12.650	23.24	192.39
Olivin-bentonite	0.217	11.715	27.38	249.74
Cerabeads-furan	0.189	8.491	58.03	652.47

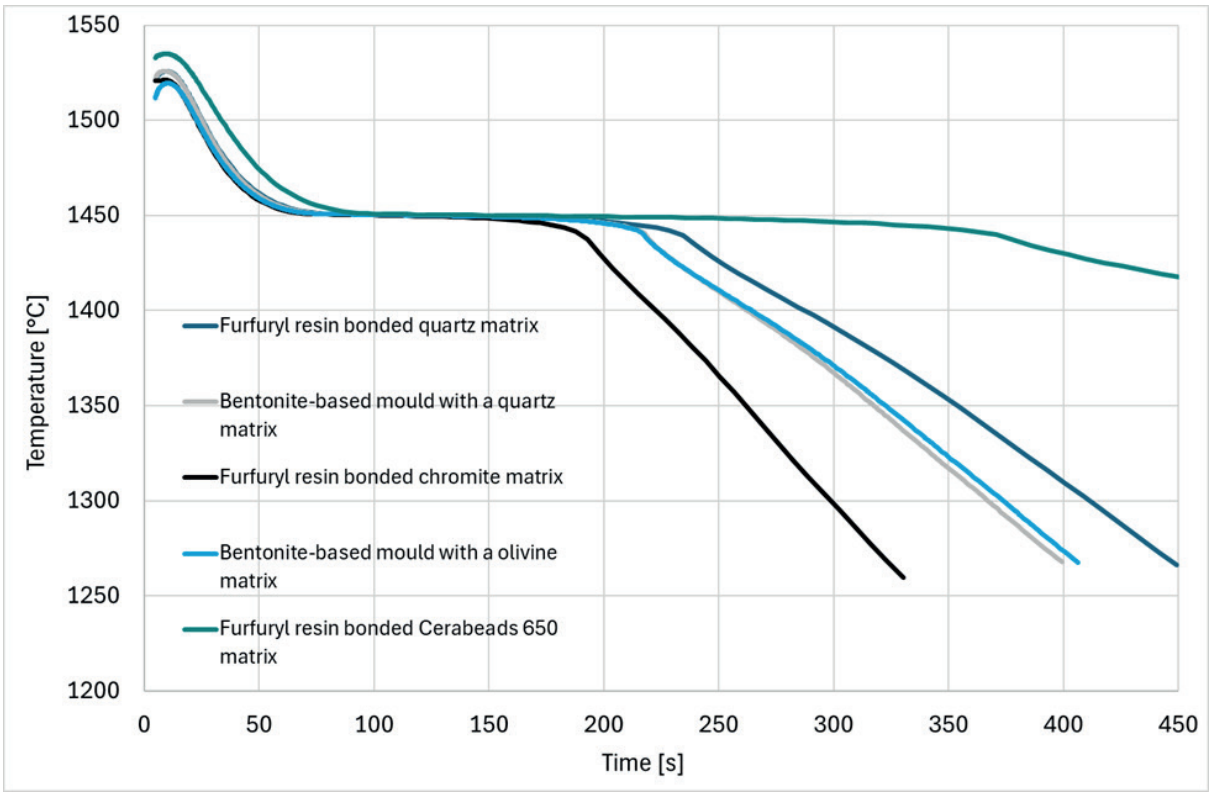

Fig. 5. The run of the cooling curves registered in the thickest part of the casting (TC_01) for different molding materials

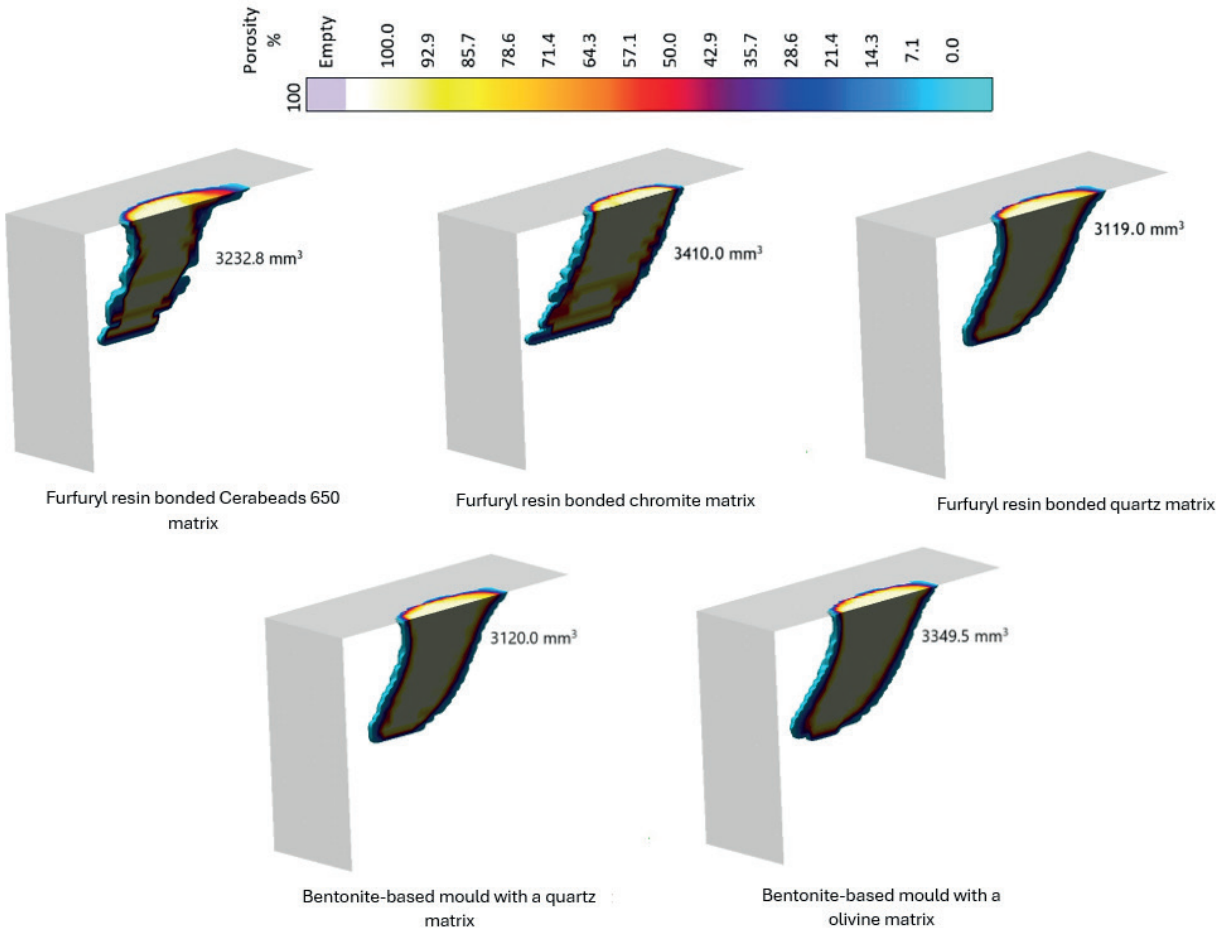

Fig. 6. Change in the shape of shrinkage porosity depending on the used molding material

4. CONCLUSIONS

The use of the MAGMASoft® simulation software enabled the design of the gating and feeding systems that ensure the production of a casting free from porosity in its functional part.

Based on the numerical experiment, it was confirmed that the type of molding material used affects the cooling rate of the casting and, consequently, its microstructure – including the morphology of shrinkage porosity volume in casting allowance. Considering economic aspects, the use of more expensive molding materials does not necessarily guarantee a more favorable microstructure – rapid cooling may result in hardening of the casting within the mold and the formation of internal stresses that lead to cracking. This observation requires further verification, and therefore, the issue of phase transformations and their influence on the final microstructure of the GX70CrMnSiNiMo2 alloy with 5% Ti addition remains open.

The results obtained from simulations based on partial differential equations require validation under real-world conditions, as the molding material properties used are generic and may not reflect actual behavior. Nevertheless, the data provide a valuable starting point and a solid foundation for the next stages of the research.

ACKNOWLEDGMENTS

We would like to thank AGH University of Krakow for supporting the project no. 16.16.170.654/B507, and Dr. Eng. Grzegorz Tęcza for providing access to unpublished research materials.

REFERENCES

[1] Muhammed M., Javidani M., Heidari M. & Jahazi M. (2023). Enhancing the tribological performance of tool steels for wood-processing applications: A comprehensive review. *Metals*, 13(8), 1460. DOI: https://doi.org/10.3390/met13081460.

[2] Tęcza G. & Sobula S. (2014). Effect of heat treatment on change microstructure of cast high-manganese hadfield steel with elevated chromium content. *Archives of Foundry Engineering*, 14(3), 67–70.

[3] Kalandyk B., Tęcza G., Zapała R. & Sobula S. (2015). Cast high-manganese steel – the effect of microstructure on abrasive wear behaviour in Miller test. *Archives of Foundry Engineering*, 15(2), 35–38. DOI: https://doi.org/10.1515/afe-2015-0033.

[4] Tęcza G. & Głownia J. (2015). Resistance to abrasive wear and volume fraction of carbides in cast high-manganese austenitic steel with composite structure. *Archives of Foundry Engineering*, 15(4), 129–133. DOI: https://doi.org/10.1515/afe-2015-0092.

[5] Tęcza G. & Garbacz-Klempka A. (2016). Microstructure of cast high-manganese steel containing titanium. *Archives of Foundry Engineering*, 16(4), 163–168. DOI: https://doi.org/10.1515/afe-2016-0103.

[6] Tęcza G. & Zapała R. (2018). Changes in impact strength and abrasive wear resistance of cast high manganese steel due to the formation of primary titanium carbides. *Archives of Foundry Engineering*, 18(1), 119–122. DOI: https://doi.org/10.24425/118823.

[7] Tęcza G. (2021). Changes in abrasive wear resistance during Miller test of high-manganese cast steel with niobium carbides formed in the alloy matrix. *Applied Sciences*, 11(11), 4794. DOI: https://doi.org/10.3390/app11114794.

[8] Tęcza G. (2022). Changes in microstructure and abrasion resistance during miller test of hadfield high-manganese cast steel after the formation of vanadium carbides in alloy matrix. *Materials*, 15(3), 1021. DOI: https://doi.org/10.3390/ma15031021.

[9] Tęcza G. (2023). Changes in abrasion resistance of cast Cr-Ni steel as a result of the formation of niobium carbides in alloy matrix. *Materials*, 16(4), 1726. DOI: https://doi.org/10.3390/ma16041726.

[10] Tęcza G. (2023). Changes in the microstructure and abrasion resistance of tool cast steel after the formation of titanium carbides in the alloy matrix. *Archives of Foundry Engineering*, 23(4), 173–180. DOI: https://doi.org/10.24425/afe.2023.148961.

[11] Wang Y., Lei T. & Liu J. (1999). Tribo-metallographic behavior of high carbon steels in dry sliding: I. Wear mechanisms and their transition. *Wear*, 231(1), 1–11. DOI: https://doi.org/10.1016/S0043-1648(99)00115-5.

[12] Fraś E. (2003). *Krystalizacja metali.* Warszawa: WNT.

[13] Stefański Z., Warmuzek M. & Boroń Ł. (2010). Opracowanie technologii produkcji „bentonitu zmodyfikowanego" przeznaczonego do wykonywania odlewów staliwnych ze szczególnym uwzględnieniem jakości ich warstwy powierzchniowej. *Prace Instytutu Odlewnictwa*, 50(2), 15–36.

[14] Holtzer M., Dańko R. & Górny M. (2016). Influence of furfuryl molding sand on flake graphite formation in surface layer of ductile iron castings. *International Journal of Cast Metals Research*, 29(1–2), 17–25, DOI: https://doi.org/10.1179/1743133615Y.0000000036.

[15] Kamińska J., Puzio S., Angrecki M. & Stachowicz M. (2020). The effect of the addition of bentonite clay to traditional sand mixtures on the surface quality of iron castings. *Journal of Ecological Engineering*, 21(1), 160–167. DOI: https://doi.org/10.12911/22998993/112505.

[16] Anton I.V., Militaru C., Ştefan E.M., Ivan N., Chişamera M. & Ripoşan I. (2009). Wall thickness-solidification features correlation of ductile iron castings under mold type influence. *Scientific Bulletin Series B: Chemistry and Materials Science University Politehnica of Bucharest*, 71(4), 115–130.

[17] Taler J. & Duda P. (2016). *Rozwiązywania prostych i odwrotnych zagadnień przewodzenia ciepła*. Warszawa: WNT.

[18] Homa M., Sornek K., Goryl W., Papis-Frączek K., Żak P., Dańko R. (2025). Numerical analysis of the prototype of the high-temperature thermal energy storage based on sand bed. *Energy*, 333, 137472. DOI: https://doi.org/10.1016/j.energy.2025.137472.

[19] Łągiewka M., Konopka Z., Zyska A., Nadolski M. (2013). Determination of heat accumulation coefficient for oil bonded molding sands. *Archives of Foundry Engineering*, 13(2), 91–94, DOI: https://doi.org/10.2478/afe-2013-0043.

[20] Lewandowski L. (1997). *Tworzywa na formy odlewnicze*. Kraków: Akapit.